J. Wind Eng. Ind. Aerodyn. 98 (2010) 253–262

Contents lists available at ScienceDirect

Journal of Wind Engineering and Industrial Aerodynamics

journal homepage: www.elsevier.com/locate/jweia

Experimental investigation on the connection between flow fluctuations and vorticity dynamics in the near wake of a triangular prism placed vertically on a plane

Guido Buresti *, Giacomo Valerio Iungo

Department of Aerospace Engineering, University of Pisa, Via G. Caruso 8, 56122 Pisa, Italy

ARTICLE INFO

Article history:
Received 22 March 2009
Received in revised form
2 July 2009
Accepted 7 October 2009
Available online 1 November 2009

Keywords:
Bluff body aerodynamics
Prisms
Wakes
Flow fluctuations
Vorticity dynamics

ABSTRACT

Experiments are carried out to investigate on the connection between flow fluctuations and dynamics of different vorticity structures in the wake of an equilateral triangular prism placed vertically on a plane with its apex edge against the incoming flow. Fluctuations at three frequencies are found to dominate in different wake regions; the highest frequency is caused by the alternate vortex shedding from the lateral vertical edges of the prism, while the lowest frequency is connected with an oscillation of the streamwise vorticity structures detaching from the free-end. The fluctuations at the intermediate frequency are shown to originate from an oscillation of the transversal vorticity sheet bounding the recirculation region behind the body. Geometrical modifications are then introduced to successively interfere with the dynamics of the different vorticity structures and thus to identify possible interactions between the various fluctuations. Indentations along the prism vertical edges produce an increase of the mean wake width and a consequent decrease of both the vortex shedding and intermediate frequencies, whereas the low-frequency fluctuations are not affected. The latter remain unaltered even when irregularities are added to the free-end edges and the streamwise vortices are seen to roll-up with a different formation process.

1. Introduction

The wakes of finite cylinders and prisms in cross-wind are dominated by the velocity fluctuations induced by the alternate vortex shedding from the body sides, but further fluctuations at different frequencies, connected with the dynamics of the vorticity structures originated by the flow passing over the body free-end, may appear in the near wake. In effect, the presence of a free-end gives rise to an intense local flow, which passes over the body tip and is deflected within the separated wake by the low pressures that are present in that region. This flow varies the width of the wake and the pressure field with respect to the two-dimensional condition, and may interact with the flow rounding the sides of the body, producing intense streamwise vortical structures. A significant interference with the regular vortex shedding mechanism may thus also be expected.

Measurements of oscillating pressures and velocity fluctuations around circular cylinders of large aspect ratio (Farivar, 1981; Ayoub and Karamcheti, 1982; Fox et al., 1993) have shown the presence, for $h/d > 10$ (where h is the cylinder height and d its diameter), of clear vortex shedding from most of the cylinder span, with Strouhal numbers of the same order as those typical of two-dimensional flow. However, a decrease of the frequency was found in a zone approaching the upper end of the cylinders, probably due to an increase in the formation length of the shed vortices. The relative extent of this zone, which is likely to be a cell with lower-frequency shedding, increases with decreasing aspect ratio, and for $h/d < \approx 5$ the vortex shedding from the whole body takes place at a frequency that is lower than in the corresponding two-dimensional case (Sakamoto and Arie, 1983).

However, for all aspect ratios, in the very upper region near the tip of the models (i.e. within the last diameter from the free-end) both pressure and velocity fluctuations no longer show a clear peak that may be associated with alternate vortex shedding. Conversely, fluctuations at much lower frequencies, i.e. at Strouhal numbers $St=fd/U \approx 0.07$–0.08 (where f is the frequency and U the free-stream velocity) were found, e.g. by Farivar (1981), Ayoub and Karamcheti (1982), Luo et al. (1996), Kitagawa et al. (1997, 2002). These fluctuations were shown by Park and Lee (2000) to be associated with a couple of counter-rotating streamwise vortices originating from the free-end, to be independent from the vortex shedding frequency, and to be prevailingly in-phase on opposite sides of the wake.

Considering bodies with fixed separation points, Buresti et al. (1998) characterized the wake flow fluctuations for triangular prisms having two different isosceles cross-sections and placed

* Corresponding author. Tel.: +39 50 2217 260; fax: +39 50 2217 244.
E-mail address: g.buresti@ing.unipi.it (G. Buresti).

0167-6105/$ - see front matter © 2009 Elsevier Ltd. All rights reserved.
doi:10.1016/j.jweia.2009.10.004

vertically on a plane, with the wind normal to the base of the cross-section or orientated against its apex edge. Four values of the aspect ratio were analysed, viz. $h/w=1$, 1.5, 2 and 3 (where w is the width of the triangular cross-section base). Alternate vortex shedding from the lateral vertical edges of the models was found to exist for all aspect ratios, even if a decrease in its regularity with decreasing aspect ratio was apparent, particularly when the incoming flow was directed against the apex edge of the prisms. For this wind orientation, the presence of counter-rotating streamwise vortices over the free-ends of all the bodies was ascertained, and further fluctuations were also found at lower frequencies than those of the lateral vortex shedding.

A LES simulation of the flow past a prism with equilateral triangular cross-section and aspect ratio $h/w=3$, orientated with its apex edge against the incoming flow, was then carried out by Camarri et al. (2006). The values of the rms wake fluctuations were found to be in good agreement with those obtained from previous hot-wire measurements, even if the simulations were carried out at a lower Reynolds number ($Re=Uw/\nu=10^4$ instead of $Re=1.5\times10^5$) and the presence of the boundary layer over the plane was neglected. Furthermore, the low-frequency fluctuations were shown to be associated with a vertical, prevailingly in-phase, oscillation of the counter-rotating streamwise vortices detaching from the body tip and of the sheets of vorticity wrapped around them. The shape of the upper boundary of the near wake was also characterized, and the vorticity sheets shed from all the edges of the prism were found to interact in a non-trivial way to give rise to a complex topology, with a striking difference between the vertical positions of the middle and lateral portions of the upper wake boundary. The role of the horizontal cross-flow vorticity component shed from the rear edge of the body free-end could also be highlighted.

In the present paper the flow field around an equilateral triangular prism with $h/w=3$ and with the free-stream directed against its apex edge is analysed. This configuration is chosen because its free-end vorticity structures are similar to those of prisms with smaller and larger aspect ratio, and the alternate vortex shedding, although influenced by the finiteness of the body, is still strong enough for possibly interacting with the free-end flow. The dominating frequencies present in the wake are first characterized, and their connection with the dynamics of different vorticity structures is then investigated. Furthermore, the results are presented and discussed of tests in which geometrical modifications along the edges of the prism are introduced in order to interfere with the evolution of the various vorticity structures, and thus to ascertain if interactions exist between the fluctuations at the corresponding frequencies.

2. Experimental set-up and procedures

The tests were carried out in the subsonic wind tunnel of the Department of Aerospace Engineering of the University of Pisa, and the experimental set-up is sketched in Fig. 1, where the used reference frame is also shown. The model has an equilateral triangular cross-section, an aspect ratio $h/w=3$ (with a base width $w=90$ mm), and is positioned vertically on a plane, where the boundary layer thickness is approximately 15 mm. The particular orientation of the prism, with its edge directed against the free-stream, is such that the dimensions of the horseshoe vortex at the base of the model are almost negligible, and, in any case, small enough to confidently assume that it cannot have a significant effect on the upper-wake flow. The wind-tunnel turbulence level is about 0.9%, and most of the tests were carried out at a Reynolds number $Re=1.5\times10^5$.

The model was connected to a support, positioned below the plane and inside a fairing. Flow visualizations were performed by

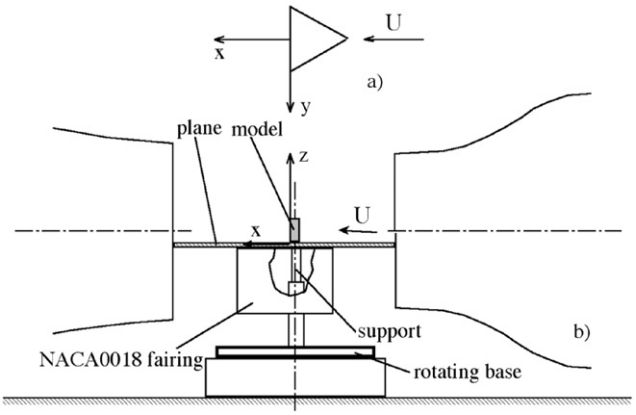

Fig. 1. Experimental set-up: (a) model orientation; (b) test lay-out.

injecting smoke upstream of the model with a probe, so that the shear layers detaching from the model edges could be highlighted; the light sheet was produced by a Magnum 1.1 Stocker Yale laser with a wavelength of ≈ 900 nm and an output power of 750 mW. As for the velocity measurements, single-component Dantec type 55 hot-wire probes and an IFA AN 1003 A.A. Lab Systems anemometry module were used. After extensive preliminary tests, a sampling frequency of 2 kHz and a time-length of approximately 33 s were chosen for the acquisitions. The probes were used with their wire orientated horizontally, and were moved in the x, y and z directions using a computer-controlled traversing rig, which allowed detailed characterizations of the wake flow field to be obtained.

Pressure measurements were also carried out, using two Pressure Systems ESP-16HD electronic pressure scanners, each with 16 ports and previously calibrated transducers. The pressure taps, about 0.5 mm in diameter, were placed over the model surfaces and connected to the respective ports through ≈ 400 mm long plastic tubes, thus assuring that the highest frequency of interest could adequately be described. From each port, signals comprising 2^{16} samples were acquired with a sampling rate of 2 kHz.

All the various dominating spectral components in the wake fluctuations are generally highly intermittent and with significant modulations, both in amplitude and frequency. The analysis of the velocity and pressure signals was then first carried out by using wavelet spectra, which are analogous but smoother than Fourier spectra for highly unsteady signals. Subsequently, a procedure based on the wavelet and Hilbert transforms, described in detail in Buresti et al. (2004), was used to extract and characterize the various dominating frequencies present in the signals. In brief, the energy wavelet maps, produced using a complex Morlet wavelet with a high value of the wavelet central frequency (to increase the frequency resolution and reduce the interference effects between adjacent components), are filtered by neglecting the wavelet coefficients outside a band centred at the frequency of interest. The inverse wavelet transform is then applied to obtain the time-series corresponding to the extracted component, which is a narrow-band signal whose modulations in amplitude and frequency may be characterized through a demodulation technique based on the construction, by means of the Hilbert transform, of its associated *analytic signal*. The time-variation of the amplitude and of the instantaneous frequency of the extracted component may thus be obtained and analysed. The instantaneous phase difference between two analogous components extracted from simultaneously acquired signals may also be obtained from their associated *cross-analytic signal* and from the *Hilbert local correlation coefficient*, *HLCC*, which varies from -1 to $+1$ and gives the

time variation of the contribution to the correlation between the two signals (see Buresti et al., 2004).

3. Results for the original prism

3.1. Flow visualizations and hot-wire measurements

Flow visualizations were first carried out on the original model to characterize the geometrical configuration of the near wake. The images obtained by setting the laser sheet in two different vertical planes orthogonal to the free-stream direction, with the camera directed upstream, are shown in Fig. 2. The visualizations largely confirm the complex upper wake flow structure highlighted from the numerical simulations of Camarri et al. (2006). In particular, the shear layers from the upstream surfaces (visualized by the smoke) are seen to wrap around two counter-rotating vortices, which detach from the front inclined edges of the free-end and whose lateral position is about $y/w = \pm 0.3$.

The visualizations obtained by positioning the laser sheet in two longitudinal vertical planes, viz. in the symmetry plane and in a plane passing through the position of the streamwise vortices, are shown in Fig. 3. The different height of the wake boundary in the two planes may clearly be appreciated; moreover, for $y=0$ the shear layer detaching from the rear edge of the free-end is seen to rapidly bend downwards inside the wake, forming the boundary of the recirculation region behind the body and apparently impinging on the rear model surface at a low vertical coordinate, similarly to what found in the LES simulation.

As for the hot-wire measurements, the velocity signals acquired aside the wake of the original prism are characterized by the presence of a spectral peak around $St=fw/U \approx 0.16$, which, through the analysis of the correlation between signals simultaneously acquired on the two sides of the wake, was shown to correspond to an alternate vortex shedding from the lateral vertical edges of the prism. The regions where this frequency (which will be denoted as HF in the following) is particularly evident are those just outside the lateral wake boundary; the latter may adequately be detected by moving the hot-wire probe from high to low absolute values of y/w, and finding the positions corresponding to a local maximum of the kurtosis of the velocity signals. The HF peak decreases in intensity moving up in the vertical direction and increases moving downstream until $x/w \approx 2.5$, which may then be assumed to roughly correspond to the formation length of the vortices. An example of wavelet spectrum obtained in a point in which this peak dominates is shown in Fig. 4a.

A lower frequency at $St \approx 0.05$ (LF in the following) is detected in the upper part of the wake, and becomes the dominating one above $z/h \approx 1.0$ and from $x/w \approx 1.5$ to 4.0 (see Fig. 4b). By using the time–frequency techniques for component extraction and cross-correlation analysis, this frequency is found to be associated with a vertical, prevailingly in-phase, oscillation of the two counter-rotating streamwise vortices detaching from the body free-end, in agreement with the numerical results of Camarri et al. (2006).

A careful analysis of all the velocity signals showed that another spectral peak at an intermediate frequency $St \approx 0.09$ (IF in the following) becomes dominant in the wake symmetry plane $y=0$, in points corresponding to different streamwise coordinates x/w depending on the vertical position; as an example, the spectrum obtained at $z/h=0.5$ and $x/w=2.5$ is shown in Fig. 4c. By comparing the positions where the IF dominates with the results of the numerical and experimental flow visualizations, the hypothesis may be made that the fluctuations at this frequency be produced by a flag-like oscillation of the sheet of transversal vorticity (i.e. the vorticity component in the y-direction) shed from the rear edge of the body free-end, and approximately lying along the downstream boundary of the recirculation region in the central part of the near wake.

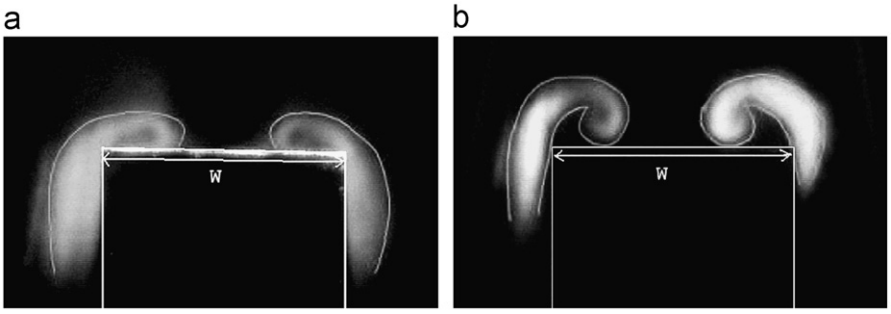

Fig. 2. Flow visualizations in vertical cross-flow planes for the original model: (a) $x/w=0$; (b) $x/w=0.25$.

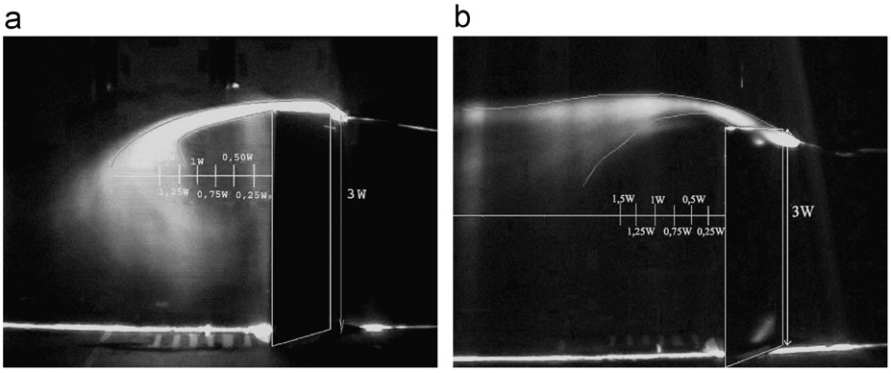

Fig. 3. Flow visualizations in vertical longitudinal planes for the original model: (a) $y/w=0$; (b) $y/w=0.3$.

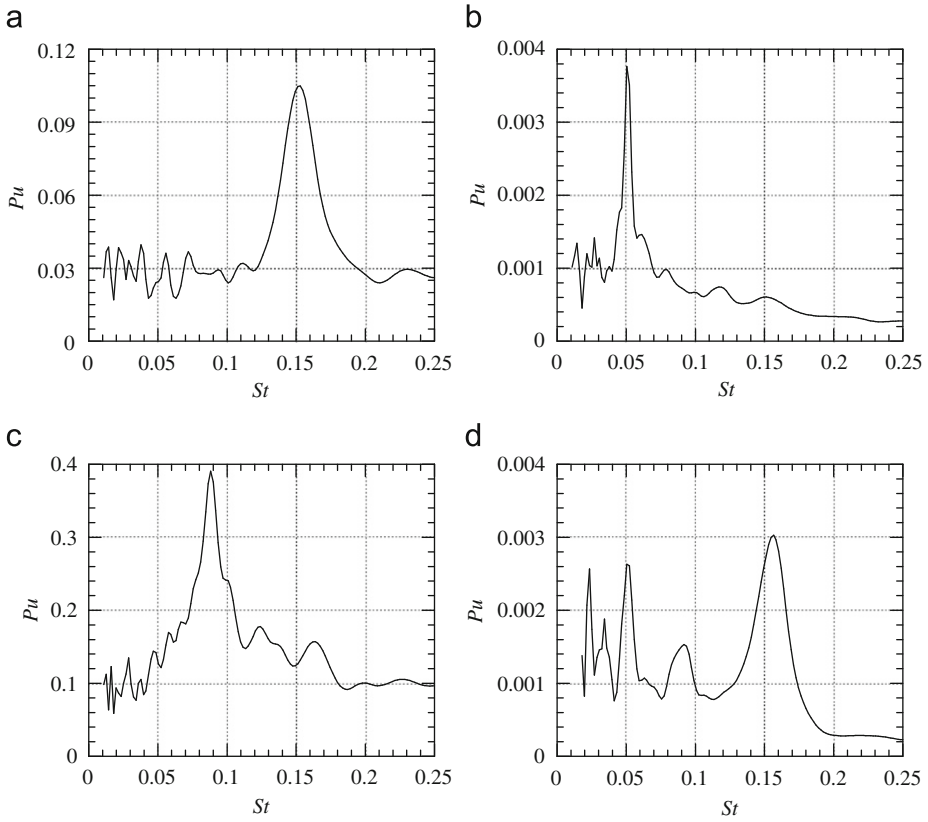

Fig. 4. Examples of the wavelet spectra obtained in various regions around the wake: (a) $x/w=2.5$, $y/w=1.0$, $z/h=0.5$; (b) $x/w=4.0$, $y/w=0.5$, $z/h=1.1$; (c) $x/w=2.5$, $y/w=0$, $z/h=0.5$; (d) $x/w=2.5$, $y/w=2.5$, $z/h=0.3$.

The three above described frequencies may also be found together in the spectra of velocity signals acquired aside the wake, sufficiently far from its boundary (Fig. 4d). In such positions the fluctuations due to vortex shedding are reduced in such a way that the peaks at the remaining frequencies become detectable. Therefore, even if the fluctuations at the various frequencies are probably produced by the dynamics of different vorticity structures, and are thus clearer near the regions where these structures are present, they all contribute to the global oscillation of the wake, which is indeed best felt further away from its boundaries.

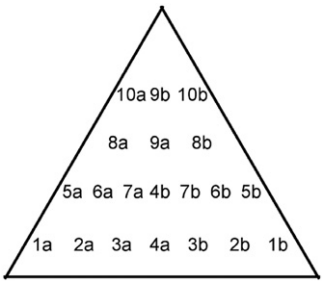

Fig. 5. Sketch of positions of pressure taps over the tip surface.

3.2. Pressure measurements

In order to substantiate the physical interpretation on the origin of the IF deriving from the analysis of the hot-wire signals, measurements of the mean and fluctuating pressures over significant parts of the model free-end and rear surfaces were carried out to single out the regions where the intermediate frequency dominates. A general view of the positions of the pressure taps placed over the free-end is given in Fig. 5, while the relevant coordinates are reported in detail in Iungo and Buresti (2007), where it is also shown that the mean values of the pressure coefficients obtained in the present investigation are in good agreement with the numerical results of Camarri et al. (2006), despite the different values of the Reynolds number.

The analysis of the fluctuating pressure signals provides more information on the dynamics of the vorticity structures originating from the free-end. In Fig. 6a the wavelet spectra of the pressure fluctuations are shown for three points along the centreline; as can be seen, the intermediate frequency (at $St \approx 0.09$) becomes dominant moving towards the rear edge of the free-end, but it is also clearly visible more upstream, together with the lower frequency (at $St \approx 0.05$) connected with the oscillation of the streamwise vortices. The IF is even stronger and more dominant on lateral points along the rear edge, as can be appreciated from Fig. 6b.

Pressure measurements on the rear surface were also carried out, using eight pressure taps on the symmetry plane $y/w=0$ from $z/h=\frac{1}{9}$ to $\frac{1}{2}$, with a mutual vertical spacing of $\Delta z/h=\frac{1}{18}$; furthermore, pressure taps were also positioned at $y/w=\pm 0.25$ and $z/h=\frac{1}{6}$, $\frac{1}{3}$ and $\frac{1}{2}$. The results of the statistical analysis of the pressure coefficients obtained on the symmetry plane are reported in Fig. 7. In this case the measurements were carried out at two different values of *Re*, and, as can be seen, the differences are not significant. The first point to be noted is that a local maximum of the mean *Cp* is clearly present between $z/h=\frac{5}{18}$ and $\frac{6}{18}$ (Fig. 7a); therefore, in agreement with the flow visualizations, this region may confidently be associated with the location where, on average,

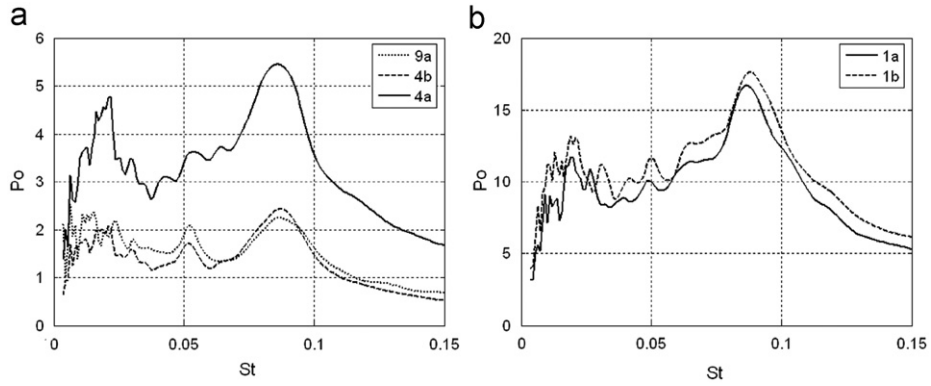

Fig. 6. Wavelet spectra of pressure fluctuations at various positions over free-end surface.

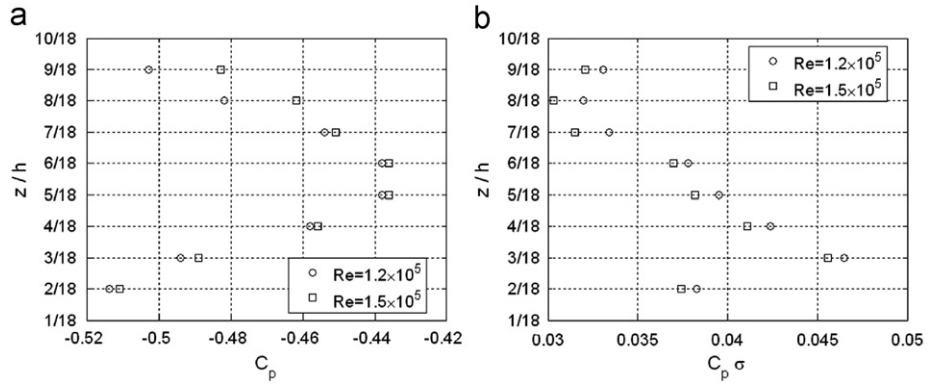

Fig. 7. Pressure coefficients over rear surface at $y/w=0$: (a) mean value; (b) standard deviation.

the transversal shear layer impinges over the rear surface. On the other hand, the maximum value of the standard deviation is found at $z/h=\frac{1}{6}$ (Fig. 7b), showing that the pressure fluctuations are definitely higher on the portion of rear surface lying just below the recirculation region.

Perhaps the most interesting result, as regards the characterization and the definition of the origin of the intermediate frequency, is the variation of the spectra of the pressure fluctuations as a function of the vertical position, which is shown in Fig. 8. In effect, the intensity of the corresponding spectral component clearly increases moving downwards, and becomes definitely dominant below the reattachment of the recirculation region. Therefore, this result, together with the prevalence of this component along the rear edge of the free-end, perfectly confirms the association of the intermediate frequency with oscillations of the sheet of transversal vorticity bounding the recirculation region behind the body.

Finally, to further characterize the fluctuating pressure field over the rear surface, the correlation between couples of pressure signals simultaneously acquired in different positions was evaluated through the method described in Buresti et al. (2004). The spectral components of interest were extracted from the two signals and their cross-correlation was obtained from the parameter *HLCC*. The procedure was applied to pairs of signals acquired either in different positions along the centreline, or in symmetrical positions on its sides (i.e. $y/w=\pm 0.25$). In all cases the median value of *HLCC* was found to be around 0.94, which suggests that the oscillations of the whole shear layer bounding the recirculation region are in phase and have a global effect, causing almost simultaneous pressure fluctuations over the rear surface. More details on the analysis of all the obtained pressure signals may be found in Iungo and Buresti (2007).

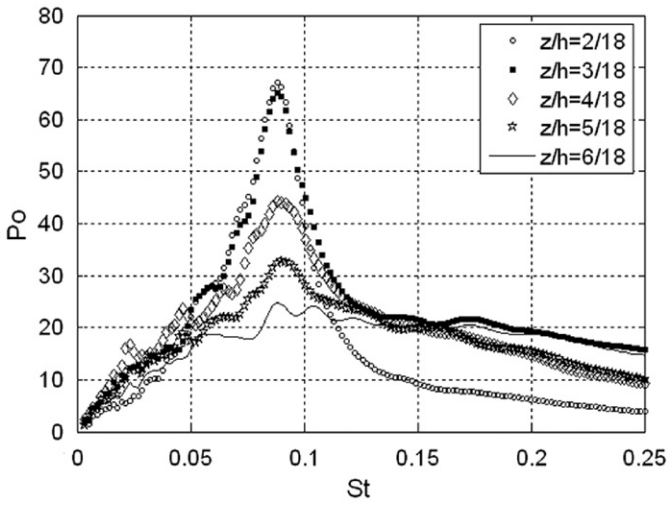

Fig. 8. Wavelet spectra of pressure fluctuations over rear surface at $y/w=0$. $Re=1.5\times10^5$.

4. Results for the modified models

4.1. Modification of the vertical edges of the prism

Having confidently established the relation between the dominating frequencies found in the wake of the prism and the dynamics of different vorticity structures, it was decided to deeper investigate on the possible interaction between the various frequencies. To this end, geometrical modifications were introduced on the model in order to successively interfere with

the dynamics of the single vorticity structures, and then check if and how the various frequencies were affected.

The first attempt was to alter, and possibly inhibit, the vortex shedding mechanism by introducing three-dimensional modifications to the lateral edges of the model. In particular, 20 mm high trapezoidal indentations were placed extending either the lateral surfaces or the rear surface (respectively, Mod1 and Mod2 in Fig. 9). On the basis of available experimental data (see, e.g. Bearman and Owen, 1998) this type of geometrical perturbation was expected to strongly hinder, or even inhibit, the regular alternate vortex shedding, and thus to modify the HF fluctuations.

In Figs. 10 and 11 the spectra of hot-wire signals from positions where the vortex shedding or the intermediate frequencies were dominant are reported for the original and modified models. As can be seen in Figs. 10a and 11a, with neither modification the frequency associated with vortex shedding disappears, even if a lowering of its value is found, which, as will be seen, is in strict connection with the increase of the mean wake width. Particularly interesting is the Mod2 case, for which, in spite of the significant geometrical disturbances introduced along the lateral edges, the vortex shedding is apparently still present, and the large widening of the wake produces much stronger fluctuations, which are felt even close to the free-end and at larger lateral distances. This is why in Fig. 11a the comparison is made for different lateral positions for the original and modified models, to allow the same scale to be used. Simultaneous measurements of the velocity fluctuations on the two sides of the wake boundary, and the analysis of the relevant hot-wire signals through the wavelet-Hilbert technique, confirmed that also for Mod2 the HF frequency is indeed related to an alternate oscillation of the wake, even if, as could have been expected, with a

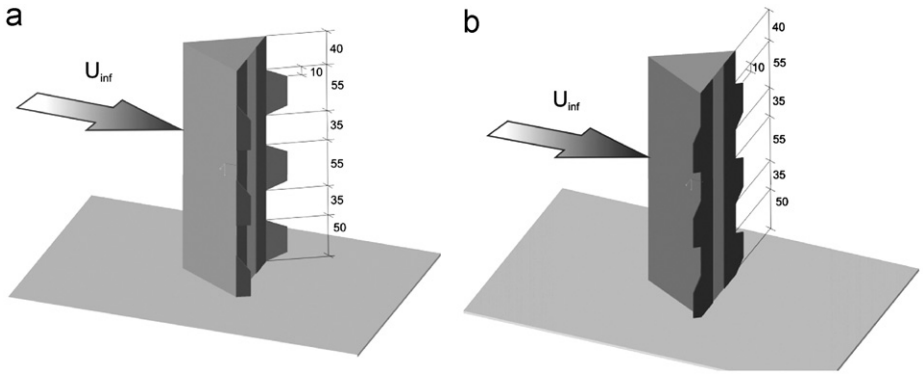

Fig. 9. Geometrical modifications to affect the alternate vortex shedding: (a) Mod1; (b) Mod2.

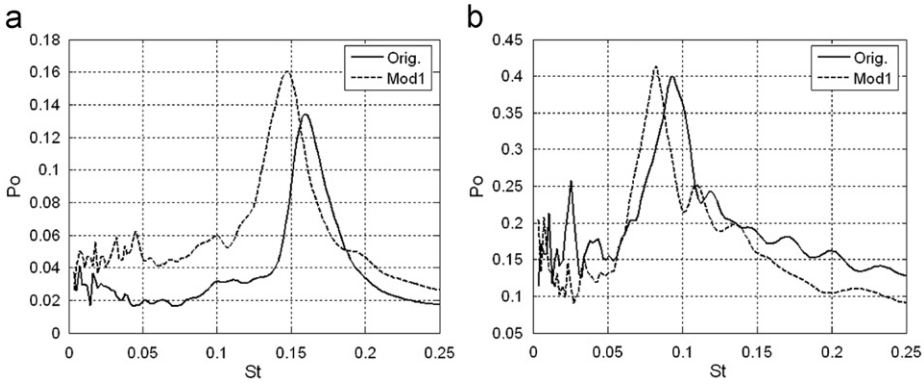

Fig. 10. Wavelet spectra for original and Mod1 configurations: (a) $x/w=4$, $y/w=-1.5$, $z/w=0.3$; (b) $x/w=2.75$, $y/w=0$, $z/w=0.4$.

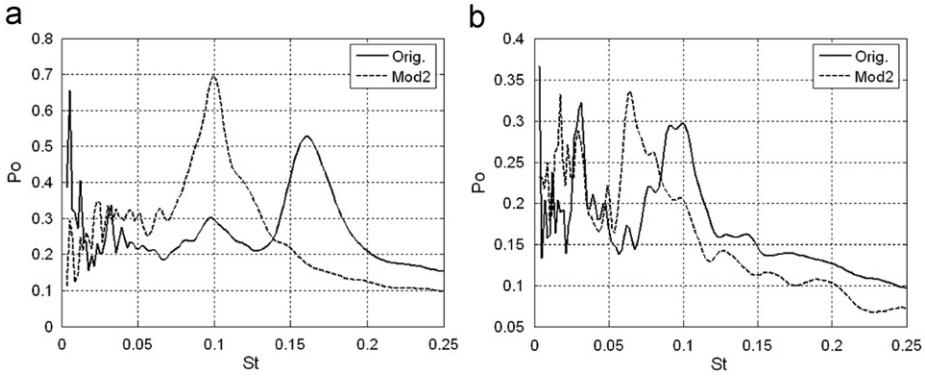

Fig. 11. Wavelet spectra for original and Mod2 configurations: (a) $x/w=2.5$, $y/w=-0.88$ (orig.), $y/w=-1.5$ (Mod2), $z/w=0.3$; (b) $x/w=2.875$, $y/w=0$, $z/w=0.3$.

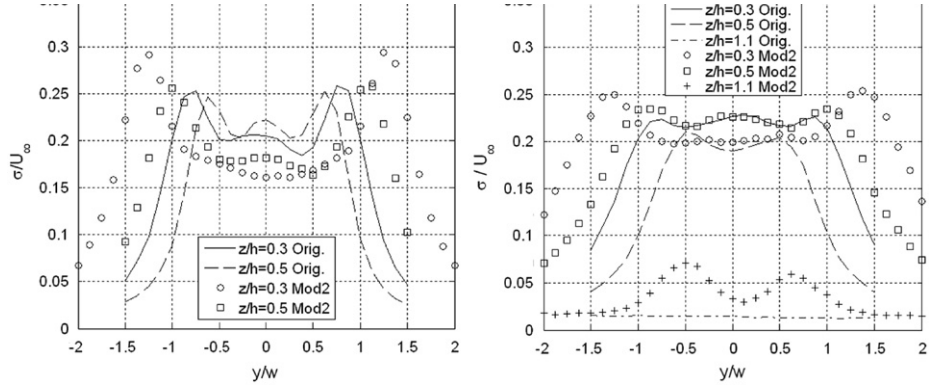

Fig. 12. Standard deviations of the *h*–w signals for the original model and Mod2: (a) $x/w=2.5$; (b) $x/w=4$.

lower level of regularity. In effect, the median values of *HLCC*, obtained using comparable procedures, were $HLCC \approx -0.94$ with a standard deviation of ≈ 0.18 for the original model, and $HLCC \approx -0.84$ with a standard deviation of ≈ 0.45 for Mod2.

To further characterize the wake variations introduced by the modifications to the lateral vertical edges of the prism, hot-wire wake surveys were carried out, which are described in detail in Iungo and Buresti (2007). The velocity standard deviations obtained at two different downstream sections and various vertical coordinates for the original model and for the Mod2 configuration are shown in Fig. 12. The significant increase of the width of the wake for the modified model is evident; furthermore, the increased fluctuations for $x/w=4$ and $z/h=1.1$ suggest that the vertical size of the wake is also increased. The Strouhal number of the HF, which was $St \approx 0.16$ for the original model, was found to change to $St \approx 0.142$ for Mod1 and to $St \approx 0.098$ for Mod2, in an almost perfect inverse relation to the increase in the mean wake width.

Considering now the connection between the various frequencies, an important point arising from Fig. 10b and 11b is that the intermediate frequency decreases roughly in proportion to the vortex shedding frequency. This result may be explained by considering that, according to the previously described physical interpretation, this frequency is connected with the oscillations of the recirculation region; now, the widening of the wake for the modified models is likely to produce a similar variation of the length of the recirculation region, which is a plausible reference length for the intermediate frequency. Anyway, particularly for the Mod2 case, the unsteadiness and modulations of this component were also found to be higher.

As for the lower frequency at $St \approx 0.05$, which had been found to dominate in the upper part of the wake, all the above described modifications did not produce any noticeable variation, thus demonstrating that it is not connected with the vortex shedding frequency or with the width of the wake. This is clearly seen from Fig. 13, where the spectra for the original and modified models, obtained at high vertical positions, are compared. This figure also shows that the fluctuations at the vortex shedding frequency for the Mod2 configuration have a much higher intensity; in effect, for this case the associated peak is clearly detectable even in this position, together with a small peak also at the intermediate frequency.

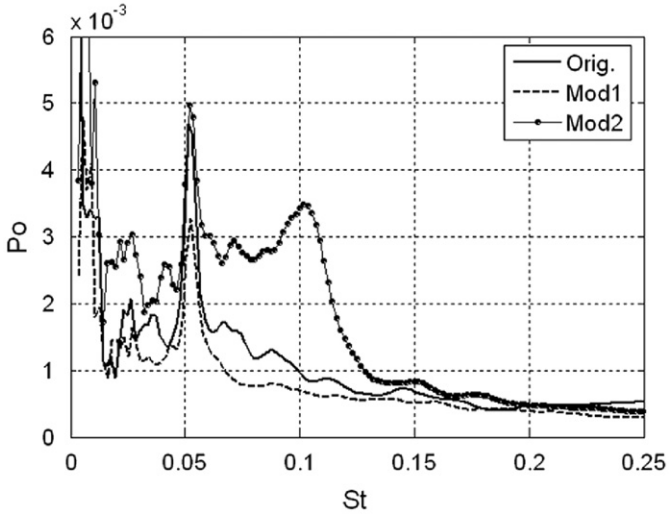

Fig. 13. Wavelet spectra for original and modified configurations: $x/w=4$, $y/w=-1.5$, $z/w=1.1$.

4.2. Modification of the free-end edges of the prism

To try to interfere with the dynamics of the vorticity structures originating from the free-end, geometrical modifications to its edges were introduced. The rear free-end edge was first modified, by adding to it triangular indentations and an elongation with a circular arc plate, in order to influence the structure of the shear layer bounding the recirculation zone, and, consequently, the intermediate frequency. The relevant results of the survey of the wake velocity fluctuations are reported in detail in Iungo and Buresti (2007), where the modified models are denoted, respectively, as Mod3 and Mod4, and where it is shown that the effects of these modifications on the wake fluctuations were definitely negligible. The fact that the HF spectral peak remained practically unaltered could perhaps be expected, as no interference with the shear layers detaching from the edges of the lateral vertical faces was introduced. But even the IF, which might have been presumed to be affected, showed virtually no change both in frequency and energy. This result may be due to the fact that these modifications did not actually vary the amount of the *y*-component vorticity being introduced in the wake, which is thus confirmed to be the important quantity driving the oscillations at the intermediate frequency. On the other hand, the invariance of the LF component is an indication that the counter-rotating streamwise vortices were not affected by the modification of the rear free-end edge.

In an attempt of directly interfering with the physical mechanism originating the low frequency, the front edges of the free-end were then modified in order to influence the roll-up of the shear layers and the formation of the free-end streamwise vortices. In particular, 10 mm high rectangular plates were added, both parallel and orthogonal to the upper surface (Mod5, Fig. 14a).

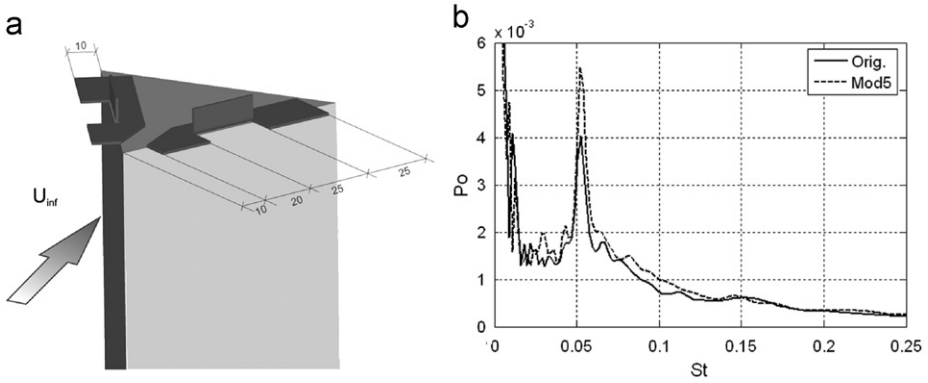

Fig. 14. Modification of free-end front edges: (a) Mod5; (b) spectra at $x/w=4$, $y/w=-1.5$, $z/w=1.1$.

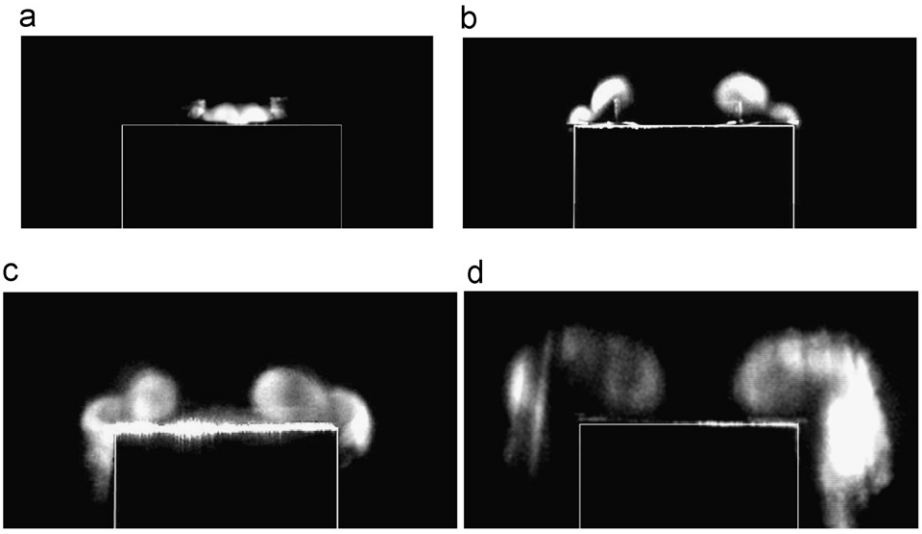

Fig. 15. Flow visualizations in vertical cross-flow planes for Mod5: (a) $x/w=-0.67$; (b) $x/w=-0.17$; (c) $x/w=0$; (d) $x/w=0.25$.

However, rather surprisingly, once again no variation was found in the frequency, energy and regularity of the fluctuations in the upper part of the wake, as may clearly be seen from the spectra of Fig. 14b. This suggests that, in spite of the significant irregularity of the free-end edges, the mechanism of roll-up of the vorticity shed from the lateral sides is still strong enough to be able to generate the streamwise counter-rotating vortices whose dynamics was considered to be responsible for the presence of the low frequency.

In order to confirm the above conjecture, and also to characterize possible differences in the formation processes of the streamwise vortices for the two cases, flow visualizations were used to compare the upper near-wake geometries of the original model and of the Mod5 configuration. Fig. 15 shows the visualizations obtained for the Mod5 model, for the same vertical planes reported in Fig. 2 and for two planes placed more upstream. The main point that can be deduced from the comparison between the two cases is that the streamwise vortices are still generated downstream of the modified model, but with a completely different formation process. In particular, smaller vortices are produced along the edges of the plates that were added on each side of the free-end. However, further downstream these vortices, which have the same sign, coalesce in a single vortex, so that, eventually, two counter-rotating vortices are produced which are comparable to those deriving from the original model, even if perhaps slightly more diffuse.

Just as interesting are the visualizations obtained by positioning the laser sheet in longitudinal vertical planes, which are shown in Fig. 16. In effect, the heights of the wake boundary in the two considered planes are similar to those of the original model shown in Fig. 3, thus confirming a comparable strength of the streamwise vortices released in the wake in the two cases. Finally, it must be pointed out that the images of the visualizations described herein are derived from digital videos which, in all the analysed cases, display the presence of further irregular oscillations of the whole recirculation region at very low frequencies.

5. Discussion and conclusions

The main purpose of this work was to investigate on the connection between flow fluctuations and dynamics of different vorticity structures in the wake of a prism with equilateral triangular cross-section, placed vertically on a plane with its apex edge against the incoming flow.

Flow visualizations confirmed the complex topology of the upper part of the near wake previously deduced from a LES numerical simulation; in particular, the shear layers from the upstream surfaces are seen to wrap around two counter-rotating vortices detaching from the front inclined edges of the free-end, and to produce a significant difference between the vertical

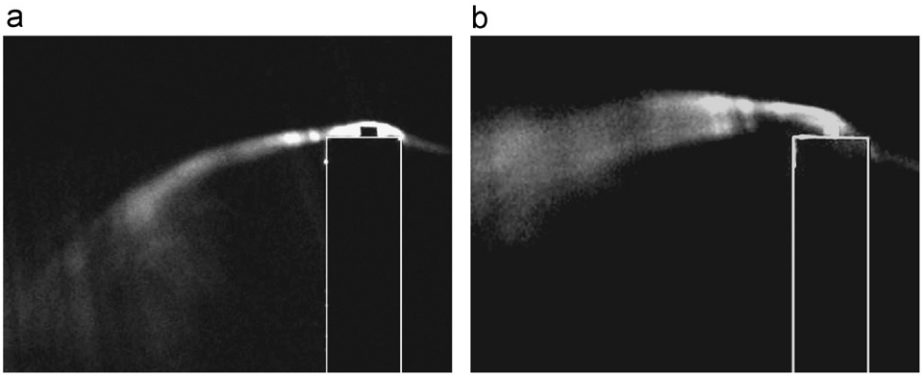

Fig. 16. Flow visualizations in vertical longitudinal planes for Mod5: (a) $y/w=0$; (b) $y/w=0.35$.

position of the middle and lateral parts of the upper boundary of the wake. Furthermore, in the central portion of the near wake a recirculation region is present, and is bounded by the shear layer formed by the transversal vorticity shed from the rear edge of the free-end, which impinges on the lower part of the rear model surface.

The presence, intensity and regions of prevalence of three different frequencies in the wake fluctuations were then characterized by means of careful hot-wire surveys. In particular, the frequency connected with alternate vortex shedding from the lateral vertical edges of the prism, with a Strouhal number $St \approx 0.16$, was found to dominate in the zones outside the lateral boundary of the wake, for vertical positions below $z/h=0.9$. A lower frequency, at $St \approx 0.05$, was found to prevail in the velocity fluctuations in the whole upper wake, for downstream distances $x/w \geq 1.5$, and was shown to be associated with a vertical, prevailingly in-phase, oscillation of the vorticity structures detaching from the free-end.

Fluctuations were also observed at an intermediate frequency $St \approx 0.09$, which was the dominant one in positions corresponding to the downstream boundary of the recirculation region in the central part of the near wake. Measurements of the mean and fluctuating pressures over the tip and rear surfaces of the model substantiate the hypothesis that the origin of this intermediate frequency be an oscillation of the transversal vorticity sheet bounding the recirculation region. Peaks at this frequency were indeed found to prevail in the spectra of the pressure signals acquired both near the rear edge of the free-end and below the reattachment point on the rear surface, over which the corresponding fluctuations were also found to be in phase.

Subsequently, geometrical modifications of the model were carried out in order to vary the evolution and dynamics of the vorticity structures originating from the edges of the prism, and thus to characterize possible interactions between the various frequencies. Trapezoidal indentations were first added to the lateral vertical edges of the model, thus introducing a considerable non-uniformity, both in model width and flow direction, along the height of the model. This was expected to hinder the production of a regular vortex shedding and to vary the HF fluctuations, so that any consequent variation of the remaining frequencies could be documented. Somewhat surprisingly, the hot-wire analysis of the wake flow fluctuations showed that strong alternate vortex shedding was still present in the modified configurations (even if with a slightly reduced regularity), and that the relevant Strouhal number decreased in close connection with the increase in the mean wake width. Incidentally, this finding is a further confirmation of the strength of the instability mechanism leading to alternate vortex shedding, and suggests that its domain of existence is definitely larger than could be expected.

As for the connection between the different fluctuations, the variation of the vortex shedding frequency was found to be accompanied by an analogous change of the intermediate frequency; this substantiates its dependence on the length of the recirculation boundary, which is likely to be proportional to the width of the wake. On the other hand, no variation of the IF was observed when the rear edge of the free-end was modified by means of indentations or of an elongation with a circular arc plate.

All the above geometrical modifications were found not to alter the lower frequency fluctuations in the upper part of the wake, which confirms that the oscillation of the streamwise vortical structures detaching from the body free-end is independent from the flow fluctuations caused by vortex shedding. Actually, this frequency remained unaltered even when the lateral edges of the free-end were made irregular by means of small rectangular plates. In effect, flow visualizations showed that in this case the near wake of the modified model is similar to that of the original prism, and that streamwise vortices are still generated from the free-end, even if with an entirely different formation process.

Acknowledgement

The financial support of the Italian Ministry of University and Research, M.U.R., is gratefully acknowledged.

References

Ayoub, A., Karamcheti, K., 1982. An experiment on the flow past a finite circular cylinder at high subcritical and supercritical Reynolds numbers. Journal of Fluid Mechanics 118, 1–26.

Bearman, P.W., Owen, J.C., 1998. Reduction of bluff-body drag and suppression of vortex shedding by the introduction of wavy separation lines. Journal of Fluids and Structures 12, 123–130.

Buresti, G., Lombardi, G., Bellazzini, J., 2004. On the analysis of fluctuating velocity signals through methods based on the wavelet and Hilbert transforms. Chaos, Solitons & Fractals 20, 149–158.

Buresti, G., Lombardi, G., Talamelli, A., 1998. Low aspect-ratio triangular prisms in cross-flow: measurements of the wake fluctuating velocity field. Journal of Wind Engineering and Industrial Aerodynamics 74–76, 463–473.

Camarri, S., Salvetti, M.V., Buresti, G., 2006. Large-eddy simulation of the flow around a triangular prism with moderate aspect-ratio. Journal of Wind Engineering and Industrial Aerodynamics 94, 309–322.

Farivar, D.J., 1981. Turbulent uniform flow around cylinders of finite length. AIAA Journal 19, 275–281.

Fox, T.A., Apelt, C.J., West, G.S., 1993. The aerodynamic disturbance caused by the free-ends of a circular cylinder immersed in a uniform flow. Journal of Wind Engineering and Industrial Aerodynamics 49, 389–400.

Iungo, G.V., Buresti, G., 2007. Experimental investigation on the wake generated from a low aspect-ratio triangular prism in cross-flow. Atti del Dipartimento di Ingegneria Aerospaziale No. ADIA 2007-4, ETS Editrice, Pisa.

Kitagawa, T., Fujino, Y., Kimura, K., Mizuno, Y., 2002. Wind pressures measurement on end-cell-induced vibration of a cantilevered circular cylinder. Journal of Wind Engineering and Industrial Aerodynamics 90, 395–405.

Kitagawa, T., Wakahara, T., Fujino, Y., Kimura, K., 1997. An experimental study on vortex-induced vibration of a circular cylinder tower at a high wind speed. Journal of Wind Engineering and Industrial Aerodynamics 69–71, 731–744.

Luo, S.C., Gan, T.L., Chew, Y.T., 1996. Uniform flow past one (or two in tandem) finite length circular cylinder(s). Journal of Wind Engineering and Industrial Aerodynamics 59, 69–93.

Park, C.-W., Lee, S.-J., 2000. Free end effects on the near wake flow structure behind a finite circular cylinder. Journal of Wind Engineering and Industrial Aerodynamics 88, 231–246.

Sakamoto, H., Arie, M., 1983. Vortex shedding from a rectangular prism and a circular cylinder placed vertically in a turbulent boundary layer. Journal of Fluid Mechanics 126, 147–165.